

InkPlay: Watercolour Simulation using the Lattice Boltzmann Method for Two-Dimensional Fluid Dynamics

Andreas Bauer
Masters Thesis MSc Computer Animation 2004/2005
NCCA Bournemouth University

Abstract

This paper describes the development of an application to simulate various artistic watercolour effects. It uses a novel fluid flow model, the Lattice Boltzmann Method for the incompressible Navier-Stokes Equation, to achieve realistic effects of ink dispersion observed in real artwork, including complex flow patterns, light fringes and boundary darkening. Unlike most previous watercolour simulations the presented solution is not concerned with interactive brush stroke input but instead creates the effect from a series of TIFF images as a post-render process to 2D and 3D animation sequences. The various parameters of the simulation and input/output options are controlled through a configuration text file.

CR Categories: I.3.3 [Computer Graphics]: Picture/Image Generation; I.6.3 [Simulation and Modeling]: Applications; J.5.0 [Computer Applications]: Arts, fine and performing.

Additional Keywords: Fluid simulation, ink, Lattice Boltzmann, non-photorealistic rendering, painting, pigments, post-render process, watercolour.

1 Introduction

As computer generated images become increasingly photo-real, recent years perhaps as a reaction saw a heightened awareness of the artistic possibilities of the medium. Artists have been using traditional media to provide information that may not be readily apparent in photographs of real life. To achieve such expressions with computer graphics is the motivation of a new field of research called non-photorealistic rendering (NPR).

Watercolour like no other medium captures the spontaneity and unpredictable nature of life itself, when the motion of water across the paper transports pigments along meandering often unexpected paths, forming streams and feathery patterns which give it its distinctive charm.

Yet because of this watercolour is perhaps the hardest natural medium to simulate as it depends heavily on the motion of the pigment solution. It is not surprising therefore that the most convincing results have been achieved using physically-based models simulating fluid dynamics.

The traditional approach to fluid simulation uses Navier-Stokes Equation solvers which calculate a given number

of individual fluid particles to simulate an overall fluid flow. This approach is computationally expensive as the quality of the simulation depends on the number of particles used with a particular challenge in the Poisson equations calculating the pressure redistribution.

An alternative method for calculating fluid dynamics has recently emerged, the Lattice Boltzmann Method, which reproduces the Navier-Stokes Equation for incompressible flows for small Knudsen and low Mach numbers.

The application developed uses the Lattice Boltzmann Method as basis for fluid physics modeling, but extends it to simulate the physics of ink flow in absorbent paper.

Fig. 1 - Sample image created with InkPlay



Simulation of brush stroke input through a sequence of 326 TIFF images.

1.1 Related work

Early watercolour paint simulations, like Strassmann's sumi-e images from 1986, Pham's flowers or Pudet's system from 1994 focus only on the recreation of brush strokes (Gooch 2001, p.31-39).

Small in 1991 and later Cockshott were the first to simulate watercolour pigment percolation by employing a cellular automaton which models watercolour paper as a two-dimensional grid of cells. But complex flow patterns were difficult to implement and required heavy computations, exposing the limitations of a pure cellular automaton approach.

Vreugdenhil in 1994 implemented a water flow model with the basic shallow water equations. These had to be

discretized in time and solved using for example Euler's method (Strohotte 2002, p.126). The influence of the paper on the flow was realized by adding conditions to the equations.

Curtis expanded Small and Cockshott's approach and incorporated some physically-based models but "by no means a strict physical simulation" (Curtis et al. 1997). But the resulting images were already much more convincing than previous approaches.

At SIGGRAPH 2005 Chu and Tai (2005) presented a real-time ink dispersion model rendering on the GPU implementing a complete physics-based fluid simulation. This paper is based on their work.

1.2 Overview

The next section describes the physical properties of watercolour and ink painting and gives examples of typical effects. Section 3 introduces the Lattice Boltzmann Method and section 4 discusses the implementation. Finally section 5 discusses observations and some ideas for future research.

2. Physical nature of watercolour and ink

Using brushes, fingers or other application methods artists create expressive lines and shapes, exploiting the interaction between water and watercolour to produce flowing shades and feathery patterns.

Any simulation of watercolour on paper needs to deal with the two basic items involved: watercolour (or ink) and paper.

2.1 Watercolour and ink

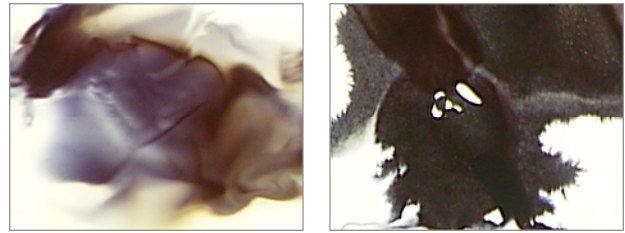
Writing ink has been used from about 2500 BC, starting in Egypt and China. It is typically a mixture of ground carbon particles combined with water and a binding agent like glue or gum. These agents provide a stable liquid suspension of pigment particles and act as a binder to fix the pigments during their application on paper to prevent them from being removed by mechanical abrasion. The higher the glue content the more viscous ink becomes.

Apart from carbon various natural dyes were used, made from metals, nuts or seeds, and sea creatures like the squid (known as sepia).

Watercolours use ground colour pigments often from precious stones. Watercolour painting began with the invention of paper in China shortly after 100 AD. In Europe watercolour was introduced in the 16th century and its earlier uses were as thin washes to colourize pen-and-ink or pencil illustrations.

Pigments can penetrate into the paper, but once in there, tend not to migrate far. Lighter pigments travel farther as they stay suspended in water longer. Carbon particles are much smaller than colour pigments and therefore seep into paper fibres easily, giving the most prominent dispersion effects.

Fig. 2 - Real watercolour effects



Left: complex flow pattern, right: boundary roughening.

2.2 Paper

Paper is mostly air, laced with a microscopic web of tangled fibres. It is typically produced from cellulose fibres extracted from various woods or plants, processed and compacted (Middleton 2003).

Chinese ink paintings typically use very thin and highly absorbent rice paper while watercolour paper is typically made from linen or cotton rags.

It is the structure of the paper that creates the striking ink effects. When faced with obstacles, water branches into streams and the flowing water carries pigments with it. Pigment diffusion plays a minimal role.

Ink dispersion is also closely determined by paper absorbency; it is the imbibition of water that causes the ink to flow through the paper fibres. To reduce absorbency, the paper can be treated with alum (Chu and Tai 2005).

3. Lattice Boltzmann Method

3.1 Historical background

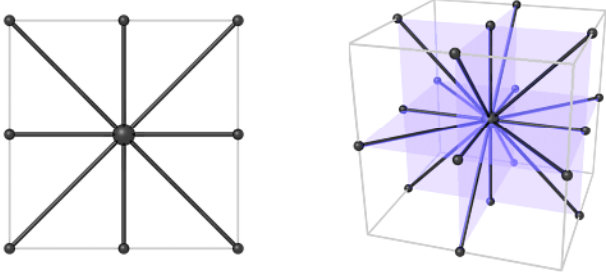
Over the last few years there has been rapid progress in the development of the Lattice Boltzmann Method (LBM) for solving a variety of fluid dynamic problems. The approach was first proposed 17 years ago by McNamara and Zanetti (1988) as an alternative to the Lattice Gas Automaton (LGA) for the numerical study of the Navier-Stokes equation.

Although the LBM shares a common origin with the LGA it overcomes the latter's shortcomings as it uses a set of real-numbered particle velocity distribution functions rather than single pseudo-particles with Boolean values. As a result the LBM does not exhibit the same noise problem as the LGA nor any of the other intrinsic flaws of Lattice Gas Automata like violation of Galilean invariance or the occurrence of large fluctuations.

(Galilean invariance is a principle which states that the fundamental laws of physics are the same in all inertial (uniform-velocity) frames of reference, i.e. all lengths and times remain unaffected by the change of velocity. (Anon 2005))

The initial variant suggested by McNamara and Zanetti (1988) was still formulated as a transcript of the lattice gas approach with a fixed fluid viscosity. By altering the collision terms in the Lattice Boltzmann Equation (LBE)

Fig. 3 - Commonly used discretization in 2D and 3D



Left: D2Q9 lattice, right: D3Q19 lattice

Bhatnagar, Gross and Krook achieved a single step relaxation scheme which replaced the discrete collision matrix that had to be formulated in the earlier model. In this new Lattice Boltzmann Bhatnagar-Gross-Krook method (LBGK) the distribution is relaxed towards a local equilibrium distribution function.

By using a Chapman-Enskog expansion it was shown that the LBGK model reproduces the Navier-Stokes Equation for incompressible fluids for low Knudsen numbers (below 0.1) and low Mach numbers (below 0.15, i.e. flow speeds below 183.75km/h (114.18mph)) (Benzi 1992).

(The Knudsen number is the ratio between the mean free molecule path and a characteristic length scale, for example an obstacle size.)

2.2 The Lattice Boltzmann Method

The LBM follows a bottom-up approach by simulating the evolution of particle distribution functions rather than particles themselves.

The LBM operates on a lattice of square or cubic cells of equal size, where each lattice site \mathbf{x} at time t stores particle distribution functions, $f_i(\mathbf{x}, t)$, along a discrete number of velocity vectors \mathbf{e}_i . In 2D space the most common variant uses 9 velocity vectors (8 neighbours and a zero vector for the cell itself) and is commonly referred to as a D2Q9 lattice. In 3D space the most common lattice models are D3Q15 and D3Q19 with 15 or 19 velocity vectors depending on whether the longest vectors point to the corners of the 3D cube (D3Q15) or to the mid point of each cube edge (D3Q19). Figure 3 shows both the D2Q9 and D3Q19 lattice.

Each distribution function f_i is stored as a floating point value and represents the probability of the presence of particles in the current cell moving in a velocity vector's direction.

During each time step Δt two operations are performed at each lattice site:

- 1.) Streaming f_i s to the next lattice site along their respective velocity vectors.
- 2.) Colliding f_i s that arrive at the same site. The colliding step subsequently computes the effect of the collisions which occur during the stream step. The

collision redistributes towards their equilibrium distribution functions $f_i^{(eq)}$.

The two operations of streaming and collision are mathematically described by the Lattice Boltzmann Equation:

$$f_i(\mathbf{x} + \mathbf{e}_i \Delta t, t + \Delta t) = (1 - \omega) f_i(\mathbf{x}, t) + \omega f_i^{(eq)}(\mathbf{x}, t) \quad \text{Eq. 1}$$

where ω is the relaxation parameter.

According to the LBGK model the equilibrium distributions $f_i^{(eq)}$ are:

$$f_i^{(eq)} = w_i \left\{ \rho + \rho_0 \left[\frac{3}{c^2} \mathbf{e}_i \cdot \mathbf{u} + \frac{9}{2c^4} (\mathbf{e}_i \cdot \mathbf{u})^2 - \frac{3}{2c^2} \mathbf{u} \cdot \mathbf{u} \right] \right\} \quad \text{Eq. 2}$$

where c equals $\Delta \mathbf{x} / \Delta t$, $\Delta \mathbf{x}$ is the lattice spacing, w_i are constants determined by the lattice geometry, ρ and \mathbf{u} are fluid density and velocity respectively, and ρ_0 is a predefined average fluid density.

For a D2Q9 lattice the constants w_i are set as 4/9 for the zero vector, 1/9 for the velocity vectors pointing north, south, east and west, and 1/36 for the diagonal velocity vectors of the lattice.

Fluid density and velocity at each site can be calculated from these values by simple summation:

$$\rho = \sum_{i=0}^8 f_i \quad \text{Eq. 3}$$

$$\mathbf{u} = \frac{1}{\rho_0} \sum_{i=1}^8 \mathbf{e}_i f_i \quad \text{Eq. 4}$$

A new set of distribution functions is obtained from a weighted average of the streamed distribution functions with the equilibrium distribution functions.

Obstacles are handled by reflecting the particle distribution functions at the obstacle boundary, resulting in a normal and tangential velocity of zero (bounce back scheme).

2.3 Advantages over Navier-Stokes Solvers

Giving the same results as the Navier-Stokes Equation (within the low Knudsen and Mach limits), Yu (2003) pointed out the following advantages of the LBM over traditional Navier-Stokes solvers:

- 1.) NS solvers need to treat the nonlinear convective term, $\mathbf{u} \cdot \nabla \mathbf{u}$; the LBM totally avoids it as the convection becomes simple advection.
- 2.) NS equations must solve the Poisson equation for pressure which are computationally expensive and involve global data communication; the LBM obtains pressure through an equation of state and data communication is always local lending itself very well to parallel computing.

- 3.) As the Boltzmann equation is kinetic-based, any physics associated with the molecular level interaction can be easier implemented in the LBM.

4. Implementation

4.1 Goal and general considerations

The key aim for InkPlay was to provide a post-render watercolour effect to existing still images or animation sequences. It was designed specifically with Ngan-Sum Tse's animation masters project in mind as she required such an effect.

This is in contrast to most watercolour implementations which usually provide some kind of graphical user interface typically a paint brush simulation.

Not having to implement a graphical user interface has the obvious time-saving advantage but there were others as well.

Chu and Tai (2005) had to cut a few corners in their watercolour simulation to be able to provide a real-time graphical user interface with a guaranteed response time of at least 40-44 frames per second. To achieve these impressive frame rates, they implemented the fluid dynamic simulation on a programmable GPU using a series of parallel rendering fragment programs. This choice makes sense as the LBM is well suited for parallel processing and this also leaves the CPU free to handle the brush simulation. But the limiting factor was the video memory. With a maximum of 256MB VRAM they could only render a simulation resolution of up to 512^2 pixel. To break this barrier for the user they employed texture scaling resizing the image to 3 or 4 times the simulation resolution and then used real-time edge sharpening techniques to re-sharpen the blurred outlines.

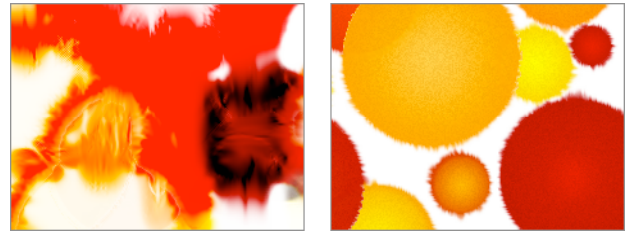
To further preserve memory and to be able to use bilinear texture interpolation Chu and Tai used 16-bit float data types (instead of 32-bit) for all simulation textures. This resulted in some precision errors.

With the decision not to implement a graphical user interface for InkPlay, real-time performance was no longer a necessity and calculations could be performed in RAM allowing for much higher simulation resolutions, only limited by RAM. This was important as Ngan-Sum Tse's animation required at least the ability to support PAL resolution images (720x576 pixel).

And being not limited by VRAM all simulation textures were implemented as 32-bit floats to avoid the precision errors Chu and Tai encountered.

For the 2D fluid dynamic simulation a D2Q9 lattice was implemented with e_0 the zero vector, e_1, e_2, e_3, e_4 the nearest neighbour sites (N, E, S, W) and e_5, e_6, e_7, e_8 pointing along the diagonals to the next nearest cells (NE, SE, SW, NW).

Fig. 4 - Artificial watercolour effects created by InkPlay



Left: complex flow pattern, right: boundary roughening.

4.2 Data input / output

4.2.1 Image input / output

Without a graphical user interface another means had to be found for data input and output. The "Tag Image File Format" (TIFF) was chosen for both image input and image output for two reasons:

- 1.) All major animation and compositing packages support TIFFs.
- 2.) The flexible TIFF header framework provides additional benefits and a route for future expansion.

One such benefit is the ability to choose from a range of compression schemes when opening or saving files. For the latter InkPlay offers the user a choice of no compression, LZW or JPEG compression.

TIFF support was implemented with the libtiff library by Sam Leffler.

InkPlay can be supplied with a TIFF image file name as parameter when launched from the command line interface. The file name must end in either '.tif' or '.tiff' to be recognized as a valid TIFF image file. InkPlay will test if the image file exists and if so analyze whether the file name includes a padded number.

If a number is found, InkPlay will assume the image file to be the first in a sequence of images and attempt to load a new image of the sequence in each consecutive simulation step. Should an image be missing in the sequence InkPlay will simply not add any image to the simulation during that simulation step. But it will increment the reference index to try loading the next image of the sequence in the following simulation step.

This ability to skip certain images in a sequence provides the user with control of when an image is to be applied to the simulation. For example when naming three images 'image_01.tif', 'image_09.tif' and 'image_21.tif' and when supplying InkPlay with the first image's file name as parameter InkPlay will apply the first image to the simulation during simulation step 1, the second image during simulation step 9 and the third image during step 21.

If no padded number was detected in the file name InkPlay will apply just this image once to the simulation and not look for further images to load. But the simulation will be continuously run on that one image.

If not specified otherwise, InkPlay saves every simulation step as an uncompressed TIFF file in a file sequence starting with 'image_0000.tif'.

4.2.2 Control input

While sufficient in some cases, mere TIFF image input does not provide enough control to direct the water-colour simulation to achieve specific, desired results.

InkPlay therefore supports configuration files and includes a complete configuration file parser and error checker. When launching InkPlay from the command line, instead of a TIFF image, a text file can also be supplied as parameter: the name of the configuration file. If InkPlay is launched without any parameter, a default configuration file, 'config.txt', is assumed and InkPlay will attempt to load a file of that name from the same folder in which InkPlay resides.

Configuration files allow full access to all simulation parameters, a total of 47, to achieve a great variety of effects. Support for configuration files also offers an easy way to save different sets of settings for later reuse.

Fig. 5 - Configuration file example

```
# This is an example config file

'Specify the image to load:
tiff_in, subfolder/image_00.tif

'Set fluid to average viscosity:
omega, 0.75

'Speed up the simulation by 85%:
speedScale, 1.85

'Set initial water velocity:
initialVelocity, 0.05, -0.3

'Exit simulation after 200 steps:
simStepExit, 200
```

Every configuration file requires at least one parameter, `tiff_in`, which specifies the TIFF image or first image of a sequence to be loaded.

InkPlay's configuration files provides the user with a reasonable amount of syntax flexibility. Parameters can be in any order and of any number as long as each parameter is on a separate line with its values comma- or semicolon-separated. Capitalisation of parameters is optional so are spaces, tabs and underscores within parameter names. Any of these variations is valid:

```
tiff_in, TIFF_IN, TIFFin, TiffIn, tiff in, TIFF in
q_2, Q_2, Q2, q2, q 2, Q 2
```

Lines can be left blank and comments can be added by starting a line with `/`, `*`, `#`, `'`, `|` or `!`.

To get a detailed description of all configuration file parameters and their syntax the user can launch InkPlay specifying `'-c'` or `'--config'` as parameter:

```
inkplay -c
```

Figure 5 shows an example of a short configuration file.

4.2.3 Information output

When a simulation is in progress InkPlay provides the user with detailed status and progress information in the command line window.

At the start InkPlay displays the approximate amount of RAM required and any warnings or errors during startup followed by a reminder of allowable keyboard input during the simulation. The ten number keys provide insight into the status of certain simulation texture and data maps by displaying their current status during the following simulation step before switching the display back to the default output. This allows the user to briefly check these parameters.

4.3 Paper layer simulation

Chu and Tai (2005) like Curtis et al. (1997) employ a three layer simulation model. Contrary to Curtis et al. who use a *shallow-water*, *pigment-deposition* and *capillary layer*, Chu and Tai's model uses a *surface*, *flow* and *fixture layer*. *Surface* and *flow layer* each have a data map for the water density (amount of water) and colour pigments. The *fixture layer* has only a data map for colour pigments.

4.3.1 Surface layer

Water, pigments and glue are deposited onto the surface layer first. From here they seep into the flow layer.

As InkPlay does not use a brush simulation, water pigments and glue are applied in a stamp- or stencil-like fashion one TIFF image at a time.

TIFF images are expected to be 8-bit RGB byte values yet all simulation data maps use 32-bit float data types hence TIFF images are first converted from byte to float:

$$pixel_{float} = pixel_{byte} / 255 \quad \text{Eq. 5}$$

And since TIFF images use an additive RGB colour model while colour pigments use a subtractive CMY colour model, TIFF images are converted from RGB to CMY before being applied to the surface layer:

$$CMY = \{C', M', Y'\} = \{1 - R, 1 - G, 1 - B\} \quad \text{Eq. 6}$$

InkPlay has full alpha channel support when reading and writing TIFF images. If a loaded image does not contain an alpha channel, the configuration file parameter `alphaFromImage` can create an alpha channel from the image itself where black is considered fully transparent. Alternatively the parameter `maskingColourRGB` can be used to specify an RGB value to be considered the transparent colour. Any existing or created alpha channel can be inverted with the `invertAlpha` parameter.

Chu and Tai (2005) did not require support for an alpha channel as theirs is a closed system. But when dealing with animation sequences support for an alpha channel is important. To provide this support, Chu and Tai's model

has been extended by a fifth channel (next to C, M, Y and glue) holding the alpha information. 'Alpha pigments' are added in sync with pigments applied to the surface layer and advected in sync with pigments moved in the flow layer. When saving TIFF images the content of this alpha layer is added as the fourth channel.

To compensate for the lack of a brush that pushes pigments into a certain direction, InkPlay allows the specification of a 2D velocity vector which is added to the simulation when a new TIFF image is applied.

To model variable paper receptivity, each pixel added is masked by the value $\max(1 - \rho / \lambda, m)$ where ρ is the water density, λ a receptivity parameter and m a base mask value.

Pigments deposited on the surface layer act as a reservoir that provides colour pigment supply to the flow layer.

4.3.2 Flow layer

Water gradually seeps in from the surface to the flow layer depending on the existing water density in the flow layer.

The amount of water supplied from the surface to the flow layer calculates as such:

$$\varphi = \text{clamp}(s, 0, \pi - \rho) \quad \text{Eq. 7}$$

where s denotes the water density in the surface layer, ρ the water density in the flow layer and π the capacity of the paper fibres.

Once φ is determined, s and ρ are updated accordingly and pigments in the flow layer, p_f , are updated according to the ratio of ρ to φ :

$$p_f = (p_f \rho + p_s \varphi) / (\rho + \varphi) \quad \text{Eq. 8}$$

4.3.3 Fixture layer

Pigments in the flow layer are gradually transferred to the fixture layer as the water dries. As real dried ink cannot be easily washed away Chu and Tai (2005) modelled this transfer to be a one-way process.

Watercolour pigments on the other hand are easier washed away even after the colour dried and it was therefore considered to change this transfer into a two-way process. But an almost similar effect can be achieved by preventing colour pigments from settling into the fixture layer in the first place. As this is easily done by changing the simulation parameters concerned (η , μ and ξ) extending the simulation was considered unnecessary.

4.4 Paper structure simulation

To accurately simulate paper irregularities Chu and Tai (2005) use three helper texture files: the *paper grain* texture, the *alum texture* and the *pinning texture map*.

The LBM does not consider medium permeability or free boundary evolution therefore Chu and Tai (2005) made several modifications to the basic Lattice Boltzmann implementation.

4.4.1 Permeability

Variable permeability makes the creation of interesting flow patterns possible. Permeability is realized by blocking the streaming process. Each site is associated with a blocking factor κ . Varying κ allows to simulate a wide range of media.

Chu and Tai (2005) use Succi's half-way-bounce-back scheme during the streaming process. Blocking is performed as if the link to each neighbouring site is partially blocked with a blocking factor $\bar{\kappa}_i$ which is set to be the average of the blocking factors of the two linked sites. The streaming step with bounce-back is mathematically described as:

$$f_i(\mathbf{x}, t + 1) = \bar{\kappa}_i(\mathbf{x}) f_k(\mathbf{x}, t) + (1 - \bar{\kappa}_i(\mathbf{x})) f_i(\mathbf{x} - \mathbf{e}_i, t) \quad \text{Eq. 9}$$

where f_k is the distribution function pointing in the opposite direction of f_i .

4.4.2 Viscosity

In the Lattice Boltzmann Equation viscosity is given by $(1 / \omega - 1 / 2) / 3$ assuming that $\Delta t = c = 1$. The lower the value for ω the higher the viscosity.

4.4.3 Paper grain texture

Voids in the paper fibres and alum deposited determine the paper permeability.

Fibre voids, or paper thickness patterns can simply be simulated by scanning a paper grain texture. This approach works better than trying to procedurally recreate paper structures. A very thin paper, e.g. rice paper, was scanned against a black background and the resulting image contrast enhanced and finally cropped to PAL resolution (720x576 pixel). This texture image, 'graintexture.tif', is provided with InkPlay. For different image resolutions another paper grain texture file needs to be prepared. In case InkPlay finds no suitable texture file, a new, blank (white) texture image is created and used. The texture file provided had been setup for tiling so that seamless stitches of any size can be created quickly if needed.

4.4.4 Alum texture

The alum texture file is used to simulate alum concentration. It can easily be created procedurally by sprinkling random white dots onto a solid black image.

InkPlay would not have to use a separate alum texture file as it could generate it afresh every time it is launched. But this would mean that exact repeatable recreations of watercolour effects become impossible. Therefore the alum texture, once created, is preserved so that InkPlay can use it the next time it is launched.

The blocking factor κ at each site is defined as:

$$\kappa = k_1 + k_2 G + k_3 A + k_4 g + k_5 h \quad \text{Eq. 10}$$

where G and A are values from the grain and alum texture, k_i are weights that define the blocking, g and h the glue concentration in the flow and fixture layers.

4.4.5 Boundary and advection

Since the effect of air is negligible, a single-phase model for water is used.

The LBM for single-phase models was originally designed for the fluid to fill the whole domain. To overcome this limitation movable boundaries are introduced, where any site can become a boundary site and vice versa. A boundary site is a wet lattice site (i.e. $\rho > 0$) with at least one dry site amongst its eight neighbours.

As the LBM model can cause negative water density for empty sites Chu and Tai (2005) reduce the advection when the water density gets low. This is done by introducing the factor ψ into equation 2:

$$f_i^{(eq)} = w_i \left\{ \rho + \rho_0 \psi \left[\frac{3}{c^2} e_i \cdot \mathbf{u} + \frac{9}{2c^4} (e_i \cdot \mathbf{u})^2 - \frac{3}{2c^2} \mathbf{u} \cdot \mathbf{u} \right] \right\} \quad \text{Eq.11}$$

$$\psi = \text{smoothstep}(0, \alpha, \rho) \quad \text{Eq. 12}$$

where α is a parameter for adjusting this effect.

4.4.6 Pinning texture

Boundary roughening, or so called 'toes', are caused by the spreading front being pinned at different points. A front is depinned when there is enough water pressure to overcome the pinning.

Chu and Tai use simple local rules to model pinning and depinning which can be efficiently integrated into the LBM.

A site is a pinning site if it is dry and the water density ρ at each of the site's eight neighbours is below a specific threshold. The four nearest neighbours (north, east, south, west) share the same threshold, denoted by σ , and the four diagonal neighbours (NE, SE, SW, NW) use $\sqrt{2} \sigma$.

The actual pinning is achieved by setting the blocking factor κ to a very high number to fully block all neighbouring links.

To model the effect of paper disorder, a third helper texture map is introduced. It is procedurally created by sprinkling light, short lines on a black background. Modulating s with this texture gives the effect of easier ink flow at certain locations and directions.

Furthermore σ is also made dependent on the glue concentration in the flow layer:

$$\sigma = q_1 + q_2 h + q_3 \text{lerp}(G, P, \text{smoothstep}(0, \theta, g)) \quad \text{Eq. 13}$$

where G and P are values from the grain and pinning textures, q_i are weights that define the roughening behaviour, and θ controls the effect of glue concentration on the appearance of toes. The lower θ the lower the glue concentration needs to be at which point the result equals the pinning texture (i.e. with no contribution from the grain map any more).

Like with the alum texture map InkPlay preserves this procedurally created map for later re-use to allow identical reproduction of its watercolour effects, if desired.

4.4.7 Pigment advection

The movement of pigments is calculated differently whether a site is becoming wet in the current simulation step or was already wet before.

For the former pigment concentration newly advected to site \mathbf{x} is:

$$p_i^*(\mathbf{x}) = \frac{1}{\rho} \sum_{i=1}^8 f_i p_i(\mathbf{x} - \mathbf{e}_i) \quad \text{Eq. 14}$$

For the latter the velocity is back-traced to find out from where the pigment arrived:

$$p_i^*(\mathbf{x}) = p_i(\mathbf{x} - \mathbf{u}(\mathbf{x})) \quad \text{Eq. 15}$$

At first look back-tracing might not seem like the best approach, but at closer inspection it does make sense:

Every lattice site has exactly one velocity vector assigned, which is the averaged, overall fluid movement derived from all f_i s. Tracing these vectors forward would break this 1:1 relationship as not every site will have one vector pointing to it. Several vectors could point to one site leaving other sites as 'holes'. How to fill them? And with what pigment colour? And if several vectors point to the same site likely some kind of equilibrium distribution equation would need to be called first, which could result in velocity vectors pointing at yet another site, and so on.

By back-tracing the velocity vectors after the f_i s were streamed the 1:1 relationship between a vector and a site is guaranteed and every site can be assigned pigments from some other site, guaranteeing no holes.

Back-tracing will likely point to an origin somewhere in the middle between four lattice grid points. To find out that positions exact pigment concentration a triple linear interpolation is done:

Given the regular 2D lattice grid points A, B, C and D (counter clockwise from bottom left) and their respective pigment concentrations a, b, c and d, and a point X somewhere within those four grid points, the back-traced pigment concentration x for point X is:

```
temp1 = lerp( d, c, X.x - D.x);
temp2 = lerp( a, b, X.x - A.x);
x = lerp( temp1, temp2, X.y - A.y);
```

To allow the user to enhance the effect of pigments moving, an additional parameter, `pfBackDistribution`, was introduced which is a factor for further redistribution of back-traced pigments.

5 Conclusion

5.1 Pigment advection speed

Once InkPlay was implemented it soon became apparent that the pigment movement was rather slow and did not produce the desired, feathery flow patterns as the equilibrium state was reached too quickly.

Merely increasing the velocity or water density did not work as most values are clamped between 0 and 1 for the calculations to work and any increase would be clamped.

To allow for more speed it was decided to decouple the velocity \mathbf{u} and streaming f_{is} from the rest of the calculations. A new parameter was introduced, `speedScale`, which is used to:

- 1.) Clamp \mathbf{u} and f_{is}
Instead of clamping values between -1 to 1 or 0 to 1, values are clamped between $-\text{speedScale}$ to speedScale or 0 to speedScale .
- 2.) 'Translate' between \mathbf{u} and f_{is} and other parameters
When deriving other parameters from \mathbf{u} or f_{is} like ρ , \mathbf{u} or f_{is} are divided by `speedScale` to bring their values back down to the 0 to 1 range.

This decoupling allows for higher pigment advection speeds and dramatically improved the visual appearance of the simulation. But it was also found that values above 1.85 - 2.0 tend to leave visual gaps between simulation steps. Values > 2.0 tend to give even less pleasing results.

In effect the speed gain of the decoupling is only in the 85-100% range, yet it is still considered a worthwhile improvement.

Fig. 6 - Still image from the title sequence of 'Spill + Gush'



Watercolour effect rendered by InkPlay.

5.2 'Spill + Gush'

A main goal for InkPlay was to provide ink spill effects for Ngan-Sum Tse's masters animation project.

She was very pleased with the final result and used many InkPlay-created effects in her masters animation project

5.3 Future Work

5.3.1 Support for random numbers

InkPlay currently does not support any random values for configuration file parameters.

This was deliberate to allow for reproducible effects. Yet in certain instances a more random approach might be desirable.

5.3.2 Normal render support

Any velocity currently applied to a TIFF image is applied as a one directional vector to the whole image. It might be desirable to have a more topologically accurate velocity vector, which matches the object depicted.

With 3D animation normal renders could provide the directional information required. But an initial test only resulted in unwanted, radial artefacts where normal vectors are too close to each other. More testing would be needed to find a good application for normal renders. Perhaps applying only the rim vectors might work better.

Figure 7 gives an example of an early normal test render.

Fig. 7 - Initial test: using a normal render



Radial artefacts appearing when applying the X and Y vector coordinates of a normal image as velocity vectors to the simulation.

5.3.3 Individual advection for each C, M and Y pigment

Currently all colour pigments are advected at the same rate and therefore pigments will never 'split' to blend into new colours. Potentially great looking effects could be created if CMY pigments would be allowed to advect individually.

As a drawback, the memory footprint would almost triple as each pigment will require its own LBM simulation.

Likely the Kubelka-Monk model would have to be used to perform the optical compositing of glazing CMY layers.

At that point it might be useful to consider switching the colour model to CMYK instead of CMY for added effects.

Acknowledgements

I would like to thank Prof. John Vince, Dr. Ian Stephenson and Dr. Stephen Bell for many helpful discussions; James Whitworth for pointing me towards useful C++ techniques; and Ngan-Sum Tse for making watercolour effects created with my application an integral part of her animation masters project.

References

ANON, 2005. *Wikipedia* [online]. Available from: http://en.wikipedia.org/wiki/Main_Page [accessed on 3 September 2005]

BENZI, R. et al., 1992. The Lattice Boltzmann Equation: Theory and Applications. *Physics Reports (Review Section of the Physics Letters)*, 222 (No. 3), 145-197.

CHU, N. S.-H. and TAI C.-L., 2005. MoXi: Real-Time Ink Dispersion in Absorbent Paper. *Proceedings of ACM SIGGRAPH 2005* [online]. Available from: <http://doi.acm.org/10.1145/1073204.1073221> [accessed on 3 September 2005]

CURTIS, C. J. et al., 1997. Computer-Generated Watercolour. *Proceedings of the 24th Annual Conference on Computer Graphics and Interactive Techniques* [online]. Available from: <http://doi.acm.org/10.1145/258734.258896> [accessed on 3 September 2005]

EBERT, D. S. et al., *Texturing & Modeling A Procedural Approach*. 3rd ed. San Francisco, California: Morgan Kaufmann Publishers.

GOOCH, B. and GOOCH, A., 2001. *Non-Photorealistic Rendering*. Natick, Massachusetts: A K Peters, Ltd.

HE, X. and LUO, L.-S., 1997. Lattice Boltzmann Model for the Incompressible Navier-Stokes Equation. *Journal of Statistical Physics*, 88, 927-944.

LANGLANDS, A., 2003. Simulating Watercolour Painting. *NCCA Bournemouth University Archive, BA Computer Visualisation and Animation Research Paper*. [copy provided by Dr. Stephen Bell.]

MCMANARA, G. R. and ZANETTI, G., 1988. Use of the Boltzmann Equation to Simulate Lattice-Gas Automata. *Physical Review Letters*, 61 (20), 2332-2335.

MIDDLETON, M., 2003. Computer Generated Ink with Frame to Frame Coherency for Animation. *NCCA Bournemouth University Archive, BA Computer Visual-*

isation and Animation Research Paper. [copy provided by Dr. Stephen Bell.]

POHL, T. et al., 2004. Performance Evaluation of Parallel Large-Scale Lattice Boltzmann Applications on Three Supercomputing Architectures. *Proceedings of the ACM/IEEE SC2004 Conference 2004* [online].

Available from: <http://ieeexplore.ieee.org/iel5/9595/30315/01392951.pdf?isnumber=30315&arnumber=1392951>
Digital Object Identifier 10.1109/SC.2004.37
[accessed on 3 September 2005]

RAABE, D., 2005. Overview on the Lattice Boltzmann Method for Nano- and Microscale Fluid Dynamics in Materials Science and Engineering. *Max-Planck-Institut für Eisenforschung GmbH* [online]. Available from: <http://www.mpie-duesseldorf.mpg.de/forschungProjekte/ProjekteGesamtMU/boltzmann/> [accessed on 3 September 2005]

STILL, M. 2002. Graphics Programming with libtiff. *IBM developerWorks* [online]. Available from: <http://www-128.ibm.com/developerworks/linux/library/l-libtiff/> [accessed on 3 September 2005]

STOCKMAN, H. W. et al., 2002. Practical Application of Lattice-Gas and Lattice Boltzmann Methods to Dispersion Problems. *Sandia National Laboratories* [online]. Available from: <http://www.sandia.gov/eeselector/gc/hws/saltfing.htm> [accessed on 3 September 2005]

STROHOTTE, T. and SCHLECHTWEG, S., 2002. *Non-Photorealistic Computer Graphics*. San Francisco, California: Morgan Kaufmann Publishers.

SUCCI, S. et al., 1989. Simulations of Three-Dimensional Flows with the Lattice Boltzmann Equation on the IBM 3090/VF. *Proceedings of the 3rd International Conference on Supercomputing* [online]. Available from: <http://doi.acm.org/10.1145/318789.318804> [accessed on 3 September 2005]

TREAVETT, S. M. F. and CHEN, M., 1997. Statistical Techniques for the Automated Synthesis of Non-Photorealistic Images. *Proceedings of the 15th Eurographics UK Conference*. Norwich, 201-210.

WEI, X. et al., 2004. Lattice-Based Flow Field Modeling. *IEEE Transactions on Visualization and Computer Graphics*, 10 (6), 719-729.
Also available from: <http://ieeexplore.ieee.org/iel5/2945/29445/01333669.pdf?tp=&arnumber=1333669&isnumber=29445>
Digital Object Identifier 10.1109/TVCG.2004.48
[accessed on 3 September 2005]

YU, D. et al., 2003. Viscous flow computations with the method of lattice Boltzmann equation. *Progress in Aerospace Sciences*, 39 (2003), 329-367.